

Article

Assessment and Simulation of Urban Ecological Environment Quality Based on Geographic Information System Ecological Index

Lusheng Che ¹, Shuyan Yin ^{1,*}, Junfang Jin ¹ and Weijian Wu ²

¹ School of Geography and Tourism, Shaanxi Normal University, Xi'an 710119, China; lsche@snnu.edu.cn (L.C.); jinjunf168@snnu.edu.cn (J.J.)

² Sichuan Institute of Metal Geologic Survey, Chengdu 611730, China; weijiannnwu@163.com

* Correspondence: yinshy@snnu.edu.cn

Abstract: The urban ecological environment is crucial to the quality of life of residents and the sustainable development of the region, and the assessment and prediction of the ecological environment quality can provide a scientific guidance for ecological environment management and improvement. We proposed a novel approach to assess and simulate the urban ecological environment quality using the Geographic Information System Ecological Index (GISEI). First, we calculated the remote sensing ecological index (RSEI) for Xi'an in 2020. Second, we selected land use data, mean annual temperature, and mean annual relative humidity as ecological indicators. We regressed these indicators on the RSEI to obtain the GISEI of Xi'an in 2020. Finally, we simulated the GISEI of Xi'an in 2030 by predicting the ecological indicators and analyzed the changes in the ecological environment quality. The results of the study show that the ecological environment quality in Xi'an in 2020 is better overall. By 2030, most of the ecological environment quality in Xi'an will be worse, and the proportion of the excellent area will decrease from 42.8% to 3.8%. The more serious ecological degradation is mainly located in the regions bordering the Qinling Mountains and the Guanzhong Plain, and the ecological environment quality in most areas of the Qinling Mountains will deteriorate from excellent to good.



Citation: Che, L.; Yin, S.; Jin, J.; Wu, W. Assessment and Simulation of Urban Ecological Environment Quality Based on Geographic Information System Ecological Index. *Land* **2024**, *13*, 687. <https://doi.org/10.3390/land13050687>

Academic Editors: Jieyong Wang, Wei Song, Yaqun Liu, Kangwen Zhu, Xuanchang Zhang and Cong Ou

Received: 3 April 2024
Revised: 12 May 2024
Accepted: 13 May 2024
Published: 14 May 2024



Copyright: © 2024 by the authors. Licensee MDPI, Basel, Switzerland. This article is an open access article distributed under the terms and conditions of the Creative Commons Attribution (CC BY) license (<https://creativecommons.org/licenses/by/4.0/>).

Keywords: ecological environment quality; RSEI; GIS; Xi'an

1. Introduction

The ecological environment is a complex system of nature, society, and economy, and the degree of harmony between regional human activities and the ecological environment can be effectively reflected in its quality status [1,2]. With rapid economic growth and urbanization, some regions are facing a series of problems in the ecological environment such as forest degradation, soil erosion, water and soil loss, and urban heat islands [3–5]. The urban ecological environment is critical to the quality of life of residents and the long-term development of the region [6]. In addition, the assessment and prediction of the ecological environment quality can provide scientific guidance for ecological environment management and improvement.

At present, studies on ecological environment quality assessment can be categorized into two types: calculating an RSEI based on remote sensing (RS) and calculating an ecological index (EI) based on a geographic information system (GIS) [7]. Among them, the RSEI is widely used due to the advantages of easy data acquisition, simple calculation methods, and objective and reliable assessment results [8–10], especially in the dynamic monitoring of ecological changes. Jing [11] used the RSEI to assess the ecological quality of the Ebi Lake wetland in Xinjiang and used the results to investigate the factors influencing the ecological quality, which provided an important basis for the ecological protection of the wetland. Gao [12] studied the spatial and temporal aspects of ecological quality in the Hami Oasis over the past 18 years using the RSEI. However, the disadvantages of

this assessment method are also obvious. It requires high-quality remote sensing images, but remote sensing images are susceptible to weather [13]. In addition, it is difficult to assess large regions because there are large temporal differences between different images, which leads to inconsistent RSEIs within a region [14]. Furthermore, the larger the study area, the more remote sensing images need to be processed, which means that the computation becomes huge [15]. Calculating EI based on GIS is a way to use ecological indicators for comprehensive evaluation [16]. This assessment method has many sources of indicators, is less disturbed, and can be used for large areas. Marull [17] took the Barcelona metropolitan area as a research case and constructed the assessment system of the ecological environmental condition in urban areas with indicators such as vegetation sensitivity index and ecological isolation index. Robati [18] considered the current ecological status of the Tehran region and determined the assessment system of Tehran's ecological quality with 10 aspects such as meteorology, natural hazards, and land use. However, the traditional method of calculating EI based on GIS relies on the selection of ecological indicators and the weights assigned to the indicators. Unfortunately, there are no standardized criteria for the selection of ecological indicators, and researchers often have subjectivity in the weights assigned to the indicators because the relationship between the indicators and the ecological environment is not clear.

To fully utilize the respective advantages of RS and GIS in ecosystem assessment, we propose a new ecosystem assessment method: GISEI. Specifically, the GISEI is a method to calculate EI objectively based on the RSEI theory using GIS technology. The application of regression analysis in ecological environment quality assessment can effectively combine remote sensing and GIS. We continue to use the theory of RSEI integrated with greenness, humidity, dryness, and temperature indices [19], where greenness and dryness can be obtained by land use types, and the humidity and the temperature can be obtained by meteorological elements. In addition, recent studies have shown that land use types [20,21] and climatic conditions [22] are themselves important factors influencing ecological conditions, thus we can select meteorological data and land use types as ecological indicators. We can then obtain the objective relationship between the ecological environment and ecological indicators to calculate the GISEI objectively by utilizing regression analysis with RSEI as the dependent variable and ecological indicators as the independent variables.

In the current research, much attention has been paid to the dynamic changes in ecological environment quality over time [23,24]. On the contrary, there is a lack of research on the prediction of future ecological environment quality. In addition, the prediction of ecological environmental quality allows managers to know the future status of the ecological environment quality and the trend of ecological environment quality change in advance to propose scientific ecological protection measures, so it is an important tool for ecological protection and environmental management. When we used the GISEI to assess the ecological environment quality, the meteorological data and the land use types were taken as ecological indicators as to whether we could simulate the future ecological environment quality by predicting these ecological indicators. Coincidentally, the prediction of land use has been widely studied, Liu [25] used the PLUS model to predict the land use pattern in 2035 under different scenarios after analyzing changes in land use in the Loess Plateau. Rong [26] calculated the carbon emission intensity per unit area of six major land use types and predicted the carbon emissions of an ecological protection scenario and natural development scenario using the PLUS model. Li [27] identified the primary areas of built-up area increase in Sanmenxia, China, by predicting carbon emissions and land use using the PLUS model. In addition, scientists have updated their climate and weather simulations and forecasts [28–30]. Currently, the Working Group on Coupled Modeling (WGCM) of the World Climate Research Program (WCRP) has released the sixth generation of CMIP [31,32], which implies more sophisticated human predictions of future weather. Ding and Peng [33] have made multi-scenario predictions of meteorology in China. Therefore, we can obtain the future ecological environment quality by predicting land use and meteorological data.

The main purpose of this study was to assess and simulate the urban ecological environment quality by the GISEI, taking Xi'an as an example. First, we assessed the current ecological environment quality in Xi'an by the RSEI and the GISEI and analyzed the current ecological environment quality status of Xi'an; then, we simulated the ecological environment quality in Xi'an in 2030 by predicting ecological indicators, and analyzed the ecological environment quality status of Xi'an in the future; and finally, we analyzed the future changes in the ecological environment quality in Xi'an by comparing the two periods.

2. Materials and Methods

2.1. Study Area

Xi'an is one of the most important cities in western China, located in the middle of the Guanzhong Plain, at $107^{\circ}40'–109^{\circ}49'E$ and $33^{\circ}42'–34^{\circ}45'N$ (Figure 1). The terrain slopes from southwest to northeast and consists mainly of the Guanzhong Plain, the Loess Plateau, and the Qinling Mountains. It is a temperate, semi-humid continental climate, with an average annual temperature of $13.0–13.7^{\circ}C$ and an average annual precipitation of 522.4–719.5 mm. Meanwhile, Xi'an is a famous ancient capital and national central city of China, a regional central city, and a new starting point of the Silk Road Economic Belt, with a long history of urban development. Xi'an's GDP reached CNY 1.15 billion in 2022, an increase of 7.5 percent over the previous year based on comparable prices. According to China's seventh national census, the permanent population of Xi'an is 11.65 million. With the population and economy growing, the local ecology is suffering with a tremendous amount of pressure.

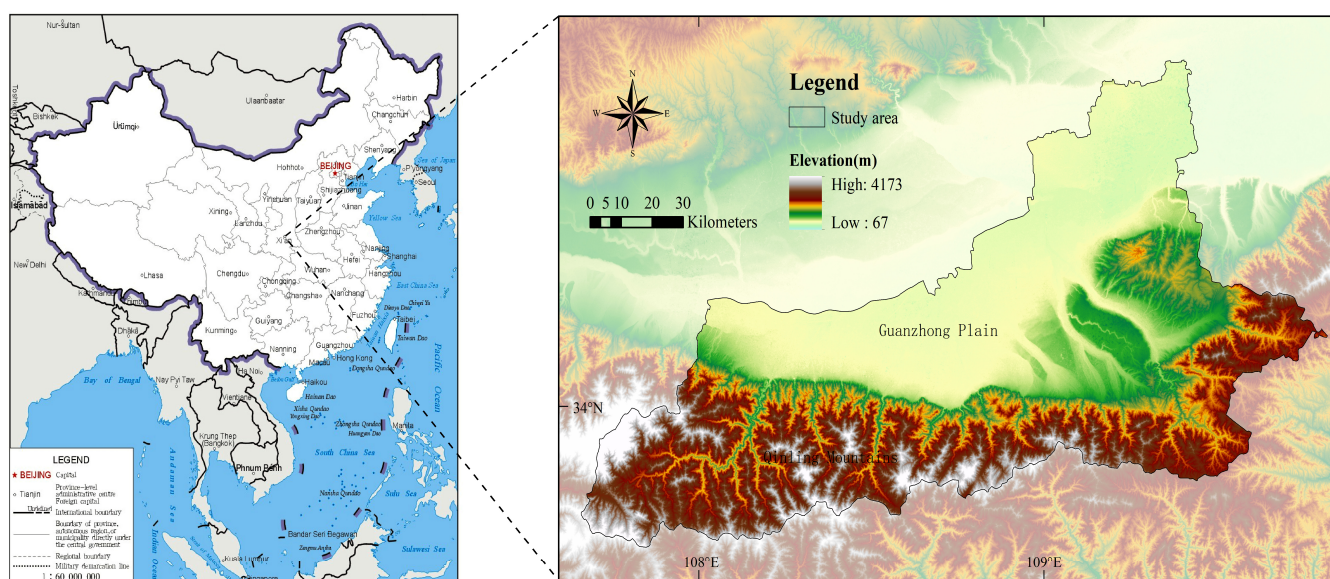


Figure 1. Geographical location and elevation of Xi'an.

2.2. Data Sources

The data used in this study are remote sensing images, land use or land cover change (LUCC), and meteorological data, all of which are publicly available, see Table 1. Ding and Peng [33] predicted meteorological data of China to 2100 based on CMIP6 under different scenarios. The data use the latest SSP scenarios released by IPCC (SSP119, SSP245, and SSP585), and each scenario includes three GCMs (EC-Earth3, MRI-ESM2-0, and GFDL-ESM4). We downloaded the temperature (monthly mean temperature) and the drought dataset under the intermediate scenario SSP245, and the MRI-ESM2-0 model in 2030, which is the dataset that is closer to the reality of Xi'an. The spatial resolution of this dataset is 0.0083333° (~ 1 km). For the mean annual relative humidity, we used the reciprocal of drought because relative humidity is inversely proportional to drought.

Table 1. Data sources.

Category	Name	Source	Explanation
Remote sensing	Landsat-8 (2020)	Geospatial data Cloud of CAS	From June to September to calculate the RSEI
LUCC	2010 and 2020	Geographic Data Sharing Infrastructure, Resource and Environment Science and Data Center	Spatial resolution is 30 m × 30 m, reclassified into six land use types: plowland, woodland, grassland, wave, construction land, and unused land
Driving Factor	DEM	Geospatial data Cloud of CAS	Spatial resolution is 30 m × 30 m
	Slope	Calculated based on DEM data using GIS platform	Spatial resolution is 30 m × 30 m
	Distance to government	National Catalogue Service for Geographic Information	Calculated by GIS spatial analysis
	Distance to road		
	Distance to railway		
	Distance to water bodies		
	GDP	Geographic Data Sharing Infrastructure, Resource and Environment Science and Data Center	Spatial resolution is 1000 m × 1000 m
	Population		
	Mean annual precipitation		
Mean annual temperature			
Soil types			
Meteorological data	Mean annual temperature (2020)	Geographic Data Sharing Infrastructure, Resource and Environment Science and Data Center	Spatial resolution is 1000 m × 1000 m
	Mean annual relative humidity (2020)	Loess Plateau Science Data Center, National Earth System	Spatial resolution is 1000 m × 1000 m
	Mean annual temperature (2030)	Science Data Sharing Infrastructure, National	Spatial resolution is 0.0083333°
	Mean annual relative humidity (2030)	Science and Technology Infrastructure of China	Spatial resolution is 0.0083333°

2.3. Research Framework

We proposed a novel approach to assess and simulate the urban ecological environment quality using the GISEI. Firstly, the RSEI for 2020 was calculated using remote sensing images, land use type, temperature, and relative humidity that were selected as ecological indicators. Second, we regressed these ecological indicators on the RSEI to calculate the GISEI for 2020. Here we used four models: ridge regression, support vector machine (SVM), random forest (RF), and BP neural network (BP) to perform the regression analysis. Third, we selected the optimal regression model using the Taylor diagram as the evaluation result. Fourth, we predicted the land use data in 2030 by the PLUS model and selected the temperature and relative humidity data in 2030 predicted based on CMIP6. After obtaining the ecological indicators for 2030, we predicted the GISEI in 2030 by an optimal regression model. Finally, we analyzed the future changes in ecological environment quality and policy-making recommendations. Figure 2 shows the detailed research framework.

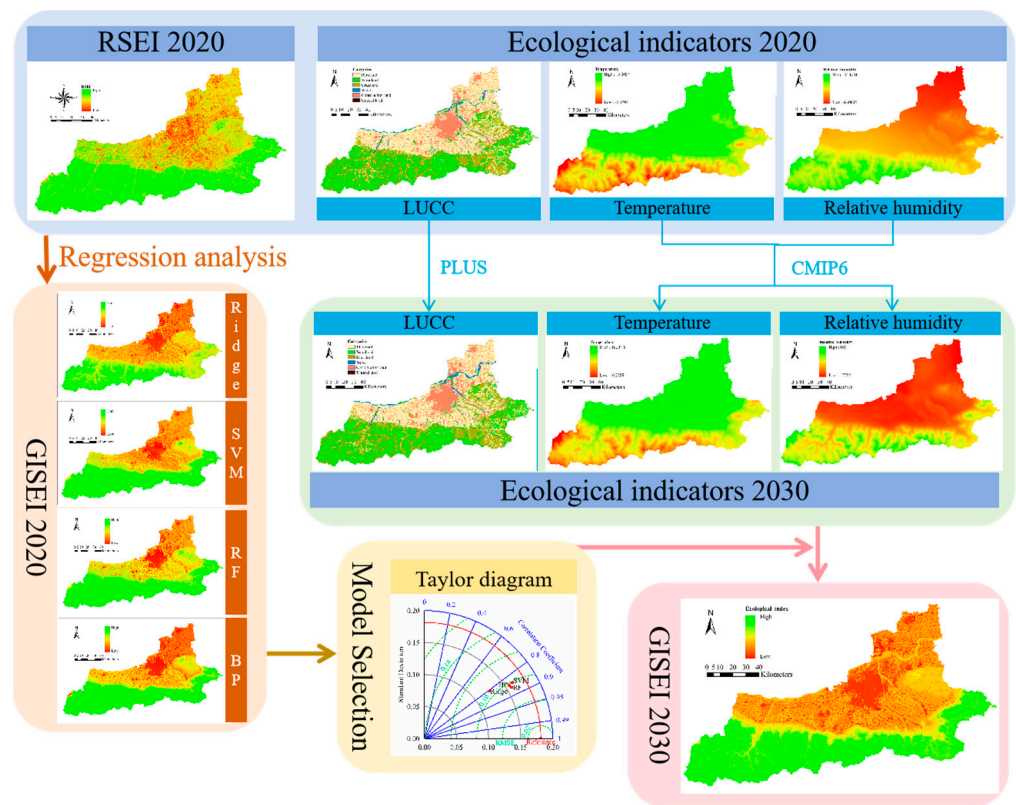


Figure 2. Research framework.

2.4. Ecological Environment Quality Assessment

We used the RSEI to calculate the GISEI to assess and simulate the ecological environment quality of the Xi’an.

2.4.1. Remote Sensing Ecological Index (RSEI)

The RSEI is often used to evaluate the quality of a local ecological environment [15,34]. To calculate the RSEI [7], the band combinations of remote sensing images were used to extract the normalized difference vegetation index (NDVI), wet index (WET), normalized difference building and soil index (NDBSI), and land surface temperature (LST), and a composite RSEI was derived from principal component analysis (PCA) for an objective and quantitative assessment [35]. Specifically, the RSEI of Landsat-8 OLI images was calculated using the following formula:

$$\left\{ \begin{array}{l}
 \text{RSEI} = f(\text{NDVI}, \text{WET}, \text{NDBSI}, \text{LST}) \\
 \text{NDVI} = (\rho_{\text{NIR}} - \rho_{\text{red}}) / (\rho_{\text{NIR}} + \rho_{\text{red}}) \\
 \text{WET} = 0.1511\rho_{\text{blue}} + 0.1973\rho_{\text{green}} + 0.3283\rho_{\text{red}} + 0.3407\rho_{\text{NIR}} - 0.7117\rho_{\text{SWIR1}} - 0.4559\rho_{\text{SWIR2}} \\
 \text{NDBSI} = \frac{(\rho_{\text{SWIR1}} + \rho_{\text{red}}) - (\rho_{\text{NIR}} + \rho_{\text{blue}})}{(\rho_{\text{SWIR1}} + \rho_{\text{red}}) + (\rho_{\text{NIR}} + \rho_{\text{blue}})} + \frac{2\rho_{\text{SWIR1}}}{\rho_{\text{SWIR1}} + \rho_{\text{NIR}}} - \left(\frac{\rho_{\text{NIR}}}{\rho_{\text{NIR}} + \rho_{\text{red}}} + \frac{\rho_{\text{green}}}{\rho_{\text{green}} + \rho_{\text{SWIR1}}} \right) \\
 \left\{ \begin{array}{l}
 \text{LST} = \gamma \times [(\varphi_1 \times L_{\text{sensor}} + \varphi_2) / \varepsilon + \varphi_3] + \delta \\
 \gamma \approx T_{\text{sen}}^2 / (b_r \times L_{\text{sensor}}) \\
 \delta \approx T_{\text{sen}} - T_{\text{sen}}^2 / b_r
 \end{array} \right.
 \end{array} \right. \quad (1)$$

where ρ_i is the reflectance of the Landsat-8 image corresponding to band i , b_r is a constant, T_{sen} is the brightness temperature detected by the sensor, L_{sensor} is the radiant luminance measured by the sensor, the calculation of φ_1 – φ_3 can be found in the reference [36], and ε is the surface-specific radiance, which is calculated from NDVI [37]. In this paper, we used Landsat-8 images from June to September 2020 to calculate the RSEI of Xi’an, because June to September is the season when the vegetation grows most vigorously, which can better

reflect the local ecological environment. First, we downloaded images with a less than 5% cloud cover and performed radiometric calibration, atmospheric correction, cropping, stitching, and fusion pre-processing operations on the images. Then, the four indices of NDVI, WET, NDBSI, and LST were calculated using the image band combinations. And finally, the RSEI was synthesized using PCA.

2.4.2. Geographic Information System Ecological Index (GISEI)

The GISEI is a method to calculate EI objectively based on the RSEI theory using GIS technology. Referring to the calculation of RSEI using greenness, dryness, temperature, and humidity, greenness and dryness can be mainly determined by land use types, and temperature and humidity can be responded to by meteorological indicators. Therefore, land use types, mean annual temperature, and mean annual relative humidity were used as ecological indicators, and these indicators and the RSEI were regression analyzed to calculate the GISEI. The GISEI can be used not only to assess current ecological environment quality, but also to simulate future ecological environment quality by predicting the ecological indicators. In this paper, we assess the ecological environment quality in 2020 and predict the ecological environment quality in 2030 using the GISEI.

2.5. Regression Analysis

Regression analysis is a predictive modeling technique that uses sample data to establish a relationship between the dependent and independent variables to obtain the value of the dependent variable that is not contained in the sample data [38]. In this study, ridge regression, support vector machine (SVM), random forest (RF), and BP neural network (BP) were used for regression analyses of RSEI and ecological indicators.

2.5.1. Ridge Regression

Ridge regression as a modification of the least squares approach [39], which abandons the requirement of unbiasedness in the least squares method from the perspective of reduced precision and loss of some information, is a regression method with biased estimation. Especially for pathological data, its regression results are reliable and realistic, suitable for data with covariance problems. In this paper, we used 1520 random sample points of plowland (x_1), woodland (x_2), grassland (x_3), wave (x_4), construction land (x_5), unused land (x_6), mean annual temperature (x_7) and mean annual relative humidity (x_8) for the ridge regression analysis with the RSEI (Y), and the results of the calculation are as follows:

$$Y = 0.77014 - 0.03x_1 + 0.07x_2 + 0.04x_3 - 0.03x_4 - 0.14x_5 - 0.05x_6 + 0.16508x_7 - 0.17339x_8 \quad (2)$$

2.5.2. Support Vector Machine

SVM is a binary classification model whose basic principle is structural risk minimization, and the SVM has developed into a supervised learning model after incorporating mathematical and statistical theory [40]. At present, the SVM is mainly used in pattern recognition, classification, regression analysis, etc. It has the advantages of fast convergence, strong generalization ability, and global optimization. In this paper, we used 1520 random sample points as the training dataset and the fishing nets as the test dataset for the SVM regression analysis; Y and X were the same as the above ridge regression.

2.5.3. Random Forest

RF grows into categorized "trees" by randomly selecting vectors through a self-help method, with each tree growing in its entirety without pruning. The variables at each node are generated from only a few random variables when the trees are generated, the variables (columns) and data (rows) are randomized, and a large number of trees generated in this randomized way are used for classification and regression, hence the name "random forest" [41]. Each tree in the forest depends on a random vector, and all vectors in the forest are independently and identically distributed. The final decision tree is generated

by “voting” on potential random vector trees, with the RF selecting the classification that receives the most votes. If the goal is regression, the mean of the results from these trees is the predicted value of the dependent variable. The RF improves the prediction accuracy without significantly increasing the computational complexity. In this paper, we used 1520 random sample points as the training dataset and fishing nets as the test dataset to perform the RF regression analysis; Y and X were the same as the above ridge regression.

2.5.4. BP Neural Network

BP is the most widely used neural network at present; it is a multi-layer feed-forward neural network, and the adjustment rule of its network weights uses the back-propagation learning algorithm with the optimal gradient descent technique; the goal is to achieve the smallest mean squared error of the network between the actual output and the desired output [42]. It has the advantages of nonlinearity, high accuracy, and good generalization performance. In this paper, we used 1520 random sample points as the training dataset and the fishing nets as the test dataset for the BP regression analysis; Y and X were the same as the above ridge regression.

2.6. Taylor Diagram

The Taylor diagram can plot the correlation coefficients, root mean square errors (RMSE), and standard deviations of multiple fields on a single polar plot, allowing for an intuitive and comprehensive assessment of the simulation capabilities and differences between multiple models [43]. The higher the correlation coefficient, the lower the RMSE, and the lower the standard deviation, which means the better the simulation. In this paper, the Taylor diagram was used to compare the simulation results of the four regression models to select an optimal regression model. Firstly, the four models were assigned values of 4, 3, 2, and 1 in the orders of standard deviation, RMSE, and correlation coefficient (Table 2). Then, the values of the four models in each aspect were summed up to obtain the comprehensive evaluation index (CEI). Finally, the model with the largest CEI was selected as the optimal regression model.

Table 2. Values of the four regression models in terms of standard deviation, RMSE, and correlation coefficient.

Model	Standard Deviation	RMSE	Correlation Coefficient	CEI
Ridge	4	1	1	6
SVM	1	2	2	5
RF	2	4	4	10
BP	3	3	3	9

2.7. Markov Chain

A random process can be reliably predicted by the Markov chain (MC) in an after effect-free manner. In addition, land use change is a random process with no consequences [44]. The Markov transfer matrix was used to determine the target year’s land-use scenarios, and MC was used to predict the changes in land-use [45]. The formula is as follows:

$$\begin{aligned}
 p(X_{t+1}|X_t, \dots, X_1) &= p(X_{t+1}|X_t) \\
 P_{n,n+1} = (P_{i,i_{n+1}}) &= \begin{bmatrix} P_{0,0} & P_{0,1} & P_{0,2} & \dots \\ P_{1,0} & P_{1,1} & P_{1,2} & \dots \\ P_{2,0} & P_{2,1} & P_{2,2} & \dots \\ \dots & \dots & \dots & \dots \end{bmatrix} \tag{3}
 \end{aligned}$$

where X_t is a set of random variables; and $P_{a,b}$ is the probability of event a moving to event b.

2.8. PLUS Model

The PLUS model is a cellular automata (CA) model based on raster data that can be used to simulate land use change at the patch scale. The model combines a rule mining method based on the land expansion analysis strategy (LEAS) and a CA model based on cellular automata of random seeds (CARS), which can be used to mine land expansion drivers and predict the patch-scale evolution of land use landscapes [46]. The LEAS module extracts the proportion of all types of land use expansion between two periods of land use change, samples from the increased proportion, and uses the random forest algorithm to mine all types of land use expansion and drivers one-by-one to determine the probability of land use development and the contribution of drivers to land use expansion. The CARS module combines random seed generation with a threshold-decreasing mechanism to simulate the automatic generation of plaques in a spatio-temporal dynamic manner, taking into account the probability of development. In addition, the PLUS model also provides land type transformation under different scenarios, such as a natural development scenario, ecological protection scenario, cultivated land protection scenario, etc. [47]. This paper aimed to find out the future ecological environment quality in Xi'an without policy intervention, and then scientifically formulate an ecological protection policy to guide the ecological environment quality to develop in a good direction. Therefore, we selected a natural development scenario to predict the land use of Xi'an in 2030.

3. Results

3.1. RSEI

We used RSEI to assess the ecological environment quality in Xi'an in 2020. The results are shown in Figure 3, from which we know that the ecological environment quality of the Qinling Mountains in the southern part of Xi'an was better than that of the plain areas. There are two main reasons for this: on the one hand, the Qinling Mountains are mostly forested, with high vegetation cover and few people living there, while the plain areas are construction land, with high building density, sparse vegetation, and where industry and population are concentrated; on the other hand, in Xi'an, the RSEI has a negative correlation with the surface temperature. The Qinling Mountains in the south have lower temperatures due to their higher elevation, while the temperature in the urban area is higher due to the urban heat island effect. Meanwhile, the RSEI identifies the ecological nuances within Xi'an well, and in general, the higher the building density and the more concentrated the population, the worse the ecological environment quality.

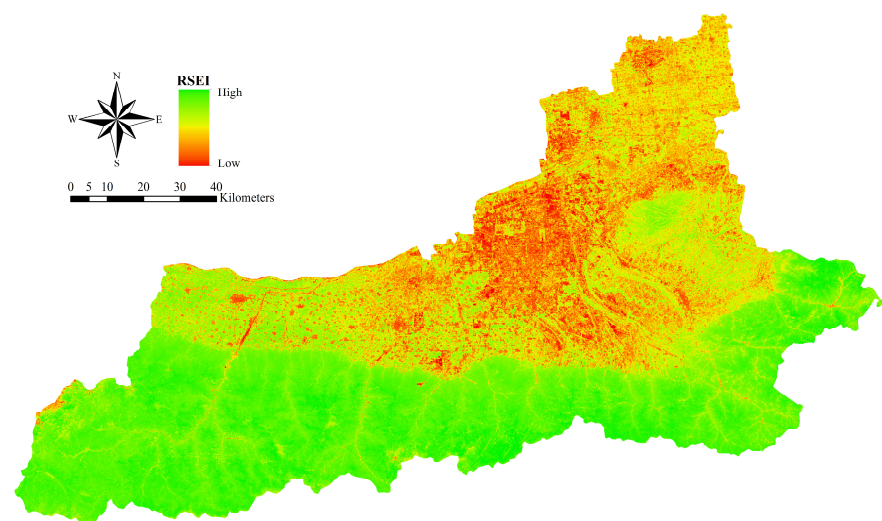


Figure 3. Spatial distribution of RSEI in 2020.

3.2. Ecological Environment Quality Assessment

The land use types were divided into six categories: plowland, woodland, grassland, wave, construction land, and unused land (Figure 4a), and we established 100×100 m fishing nets to calculate the area of each land use type within each fishing net. Meanwhile, the mean annual temperature (Figure 4b) and mean annual relative humidity (Figure 4c) with a resolution of 100×100 m were obtained by the interpolation method, and the mean annual temperature and mean annual relative humidity of each fishing net could be obtained by a superposition analysis. Similarly, the RSEI of each fishing net was analyzed by the superposition analysis. It is worth noting that the number of fishing nets was huge, and for convenient calculation, we created 1520 random points (Figure 4d) as sample data, which were analyzed in superposition with the fishing nets to obtain random sample points. Thus, each random sample point included these attribute data: the RSEI, the area of each land use type, the mean annual temperature, and the mean annual relative humidity.

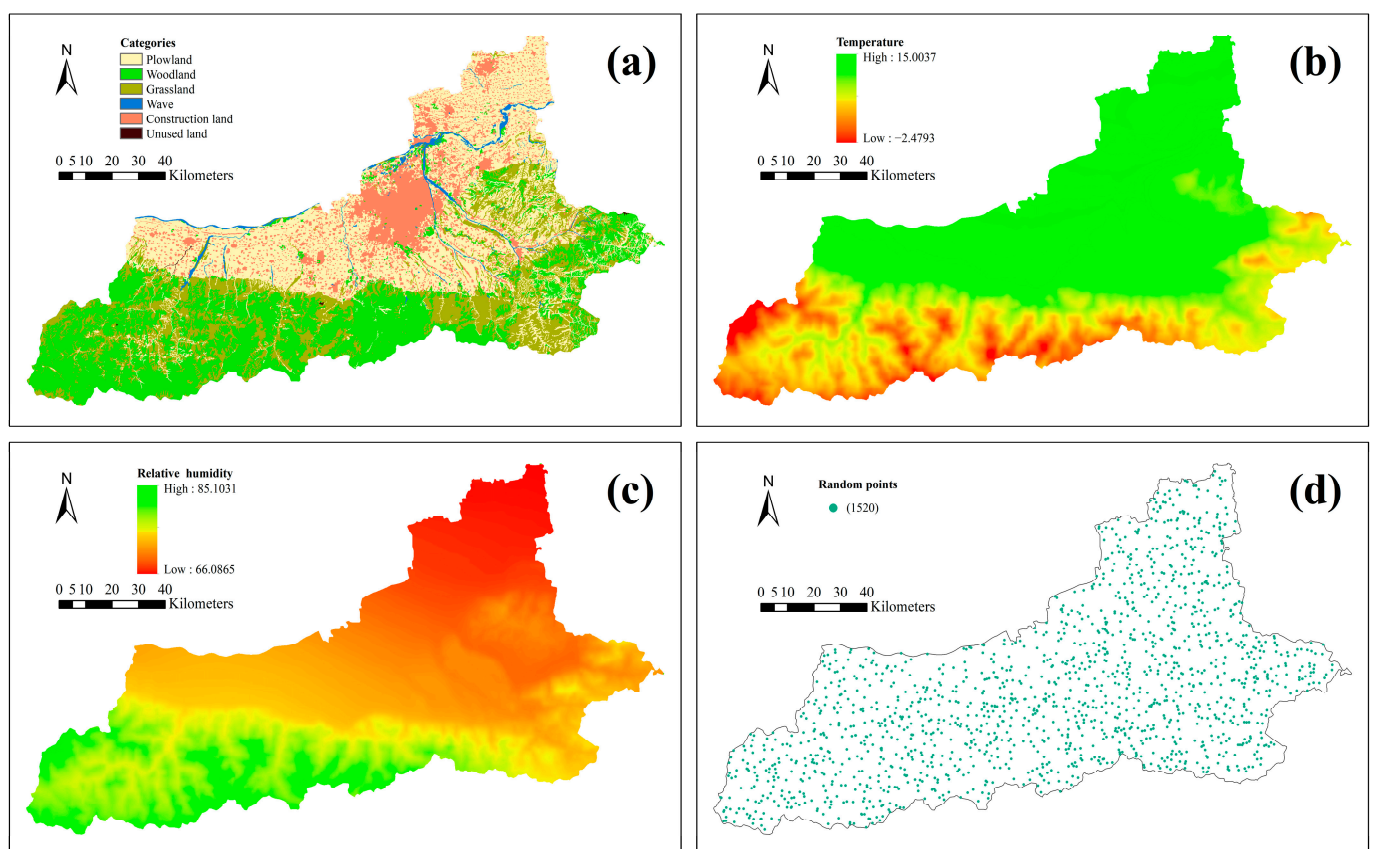


Figure 4. Ecological indicators in 2020 and random sample points: (a) land use categories; (b) mean annual temperature; (c) mean annual relative humidity; (d) random sample points.

Finally, we performed regression analyses using four models: ridge regression, SVM, RF, and BP. Specifically, we used the RSEI as the dependent variable and the area of each land use type, mean annual temperature, and mean annual relative humidity as the independent variables. The results are shown in Figure 5, where we can see a few subtle differences in the results calculated by the four regression models. The next step was to choose an optimal regression model.

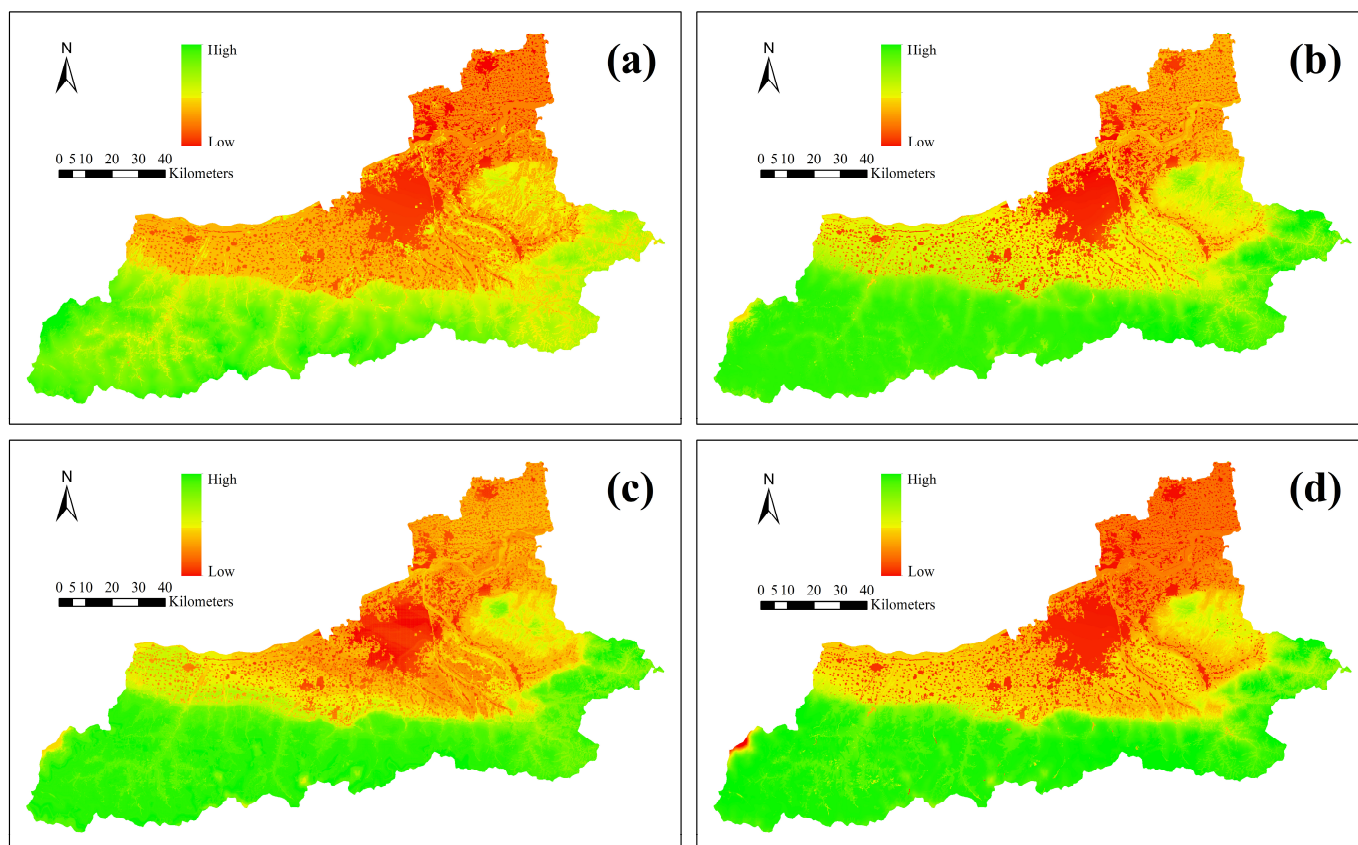


Figure 5. Spatial distribution of GISEI from regression analysis in 2020: (a) ridge regression; (b) support vector machine; (c) random forest; (d) BP neural network.

3.3. Model Selection

We have obtained four groups of GISEI values through regression analysis, and to select an optimal regression model, i.e., the GISEI was closest to the RSEI, we used the Taylor diagram to evaluate them. Specifically, we calculated the standard deviation, RMSE, and correlation coefficient between each group of GISEI and RSEI and plotted the polar plot (Figure 6). From the figure, we can see that in terms of the standard deviation, Ridge > BP > RF > SVM; in terms of the RMSE, RF > BP > SVM > Ridge; and in terms of the correlation coefficient, RF > BP > SVM > Ridge. According to the calculation, the CEI of the RF was the largest, so the RF was the optimal regression model in the regression analysis for RSEI and ecological indicators.

3.4. Ecological Environment Quality Prediction

The prediction of ecological environment quality is a guiding significance for ecological security management. In this paper, we predicted the ecological environment quality in Xi'an in 2030. First, we predicted these ecological indicators. Then, we use the relationship between ecological indicators and RSEI obtained from the RF regression analysis in the previous paper to simulate the future GISEI.

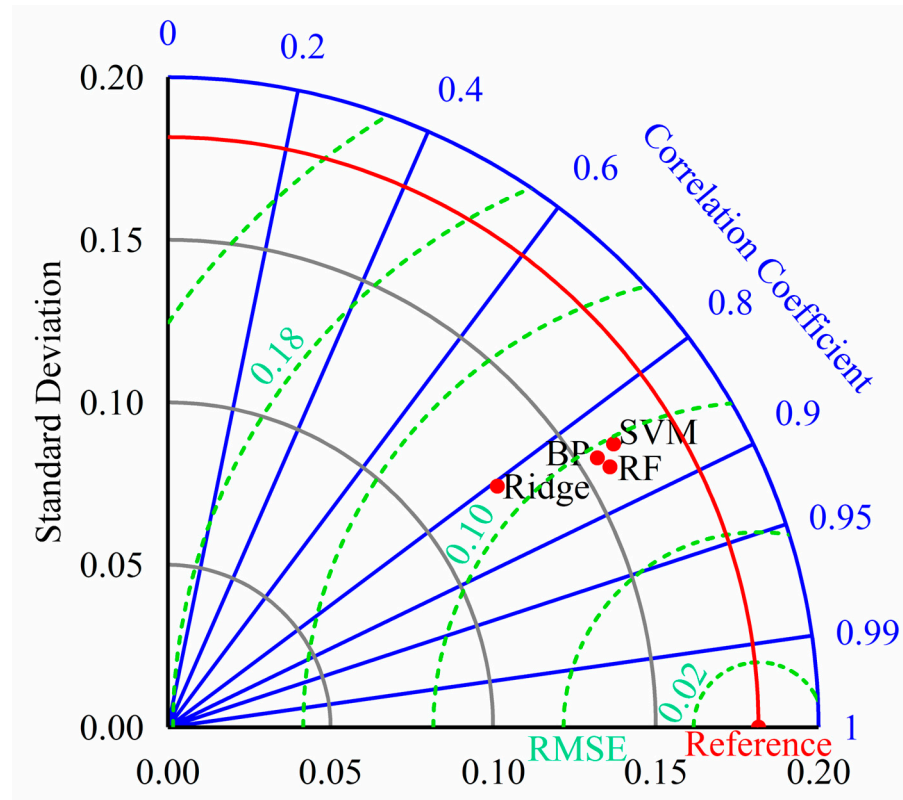


Figure 6. Taylor diagram about four regression models.

3.4.1. LUCC Prediction

In this paper, we used Patch-generating Land Use Simulation Model Software 1.4 to predict the land use changes in Xi’an in 2030. The main steps are as follows: First, the total amounts of various land use types of Xi’an in 2030 are predicted using the Markov chain based on the land use data of 2010 and 2020, and the result is shown in Table 3. Second, the land expansion analysis is conducted based on the land use data of 2010 and 2020. Third, we considered DEM, slope, distance to government, distance to roads, distance to railways, distance to water bodies, GDP, population, mean annual precipitation, mean annual temperature, and soil types as driving factors to analyze land expansion. Finally, the spatial distribution of land use types in 2030 is simulated based on the land expansion analysis strategy (Figure 7a).

Table 3. Total amounts of land use types of Xi’an in 2030.

Year	Plowland	Woodland	Grassland	Wave	Construction Land	Unused Land
2010	3,793,914	3,098,105	2,047,794	139,937	1,151,608	3513
2020	3,583,530	3,061,949	2,126,329	164,354	1,292,107	4560
2030	3,397,372	3,030,416	2,202,182	186,743	1,410,792	5324

3.4.2. Meteorological Data Prediction

The temperature and drought dataset was clipped to follow the Xi’an boundary, and we averaged the 12-month temperature data for 2030 to obtain the mean annual temperature for Xi’an. For the mean annual relative humidity, we used the inverse of drought because relative humidity is inversely proportional to drought. Then, we used the interpolation method to obtain the mean annual temperature (Figure 7b) and mean annual relative humidity (Figure 7c) at 100 × 100 m resolution of Xi’an in 2030. We found that the climate of Xi’an will be hotter and drier in 2030.

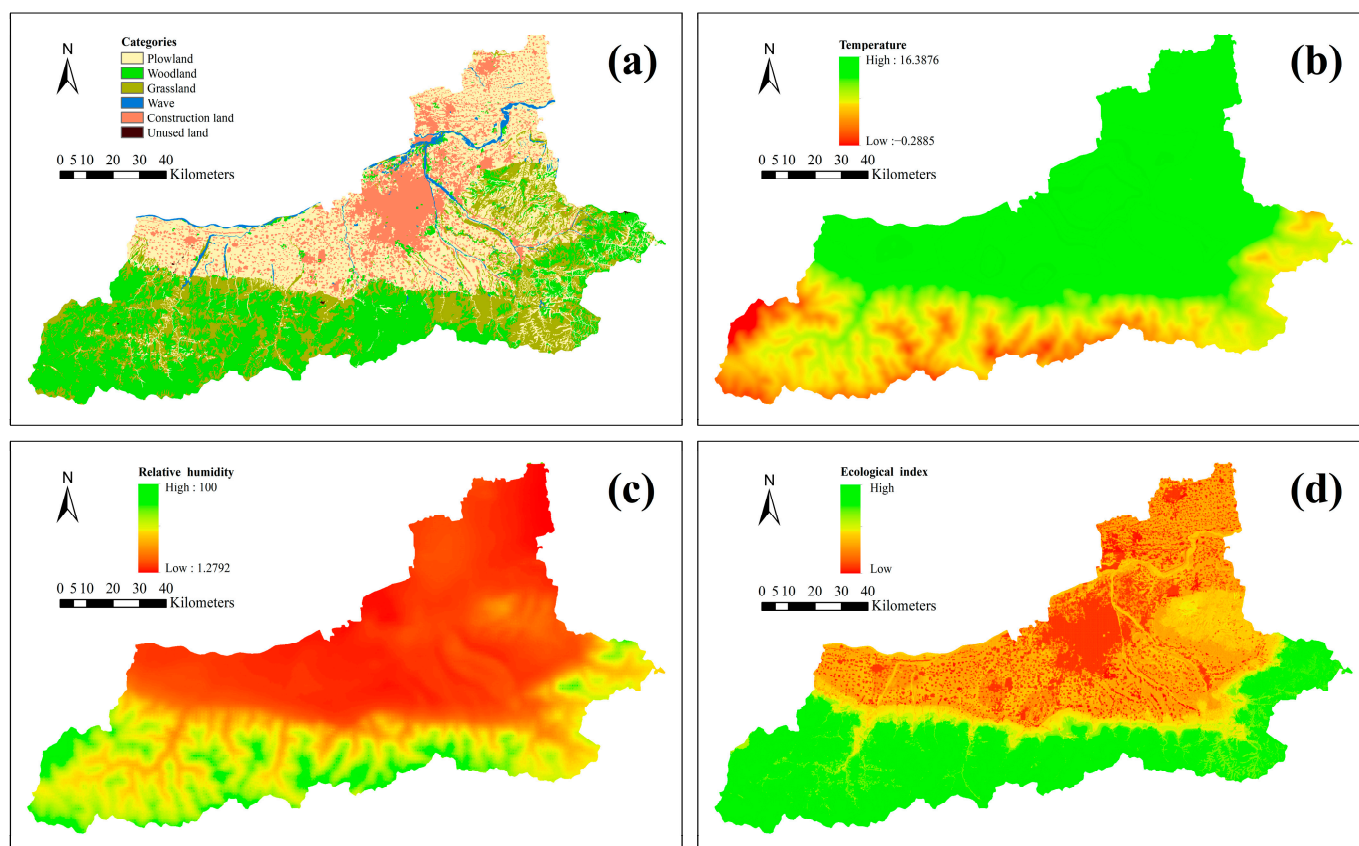


Figure 7. Ecological indicators and spatial distribution of GISEI in 2030: (a) land use categories; (b) mean annual temperature; (c) mean annual relative humidity; (d) spatial distribution of GISEI.

3.4.3. Ecological Environment Quality in 2030

After predicting the land use data and meteorological data of Xi'an in 2030, we built 100×100 m fishing nets to record the ecological indicators in 2030. Then, we calculated the areas of the six land use types, mean annual temperature, and mean annual relative humidity for each fishing net, and the order of the fields was the same as the order of the fields in 2020. Then, we used RF regression analysis to calculate the GISEI of Xi'an in 2030. Specifically, the random sample points of 2020 from the previous paper were used as the training dataset and the fishing nets in 2030 as the test dataset to perform the RF regression analysis to obtain the GISEI of each fishing net in 2030, i.e., the spatial distribution of the GISEI of Xi'an in 2030 (Figure 7d). The lower the GISEI value, the worse the ecological environment quality, we can see that in 2030, the overall ecological environment quality in Xi'an is worse, and most of the ecological environment quality of the Guanzhong Plain shows a poor value. Only the Qinling Mountains still have a good ecological environment quality, although this area covers only a relatively small area of Xi'an.

3.5. Ecological Environment Quality Change

To study the changes in the ecological environment quality in Xi'an from 2020 to 2030, we classified the GISEI obtained from the RF regression analysis in 2020 into five levels (poor, fair, moderate, good, and excellent) according to the natural breakpoint method. As shown in Figure 8a, the overall ecological environmental quality of Xi'an City shows a gradual deterioration from south to north, among which, poor accounts for 9%, mainly distributed in the central part of Xi'an, where buildings are dense and the population is densely populated; Fair accounts for 25%, which was mainly distributed in the central and northern parts of Xi'an; Moderate accounts for 13.8%, which was mainly distributed around the fair; Good accounts for 9.4%, which was mainly distributed in the areas bordering

the Qinling Mountains and Guanzhong Plain in the south of Xi’an and a small amount in the Qinling Valley area; Excellent accounts for 42.8%, which was mainly distributed in the Qinling Mountains in the south of Xi’an. In short, the overall quality of the ecological environment in Xi’an during this period was good.

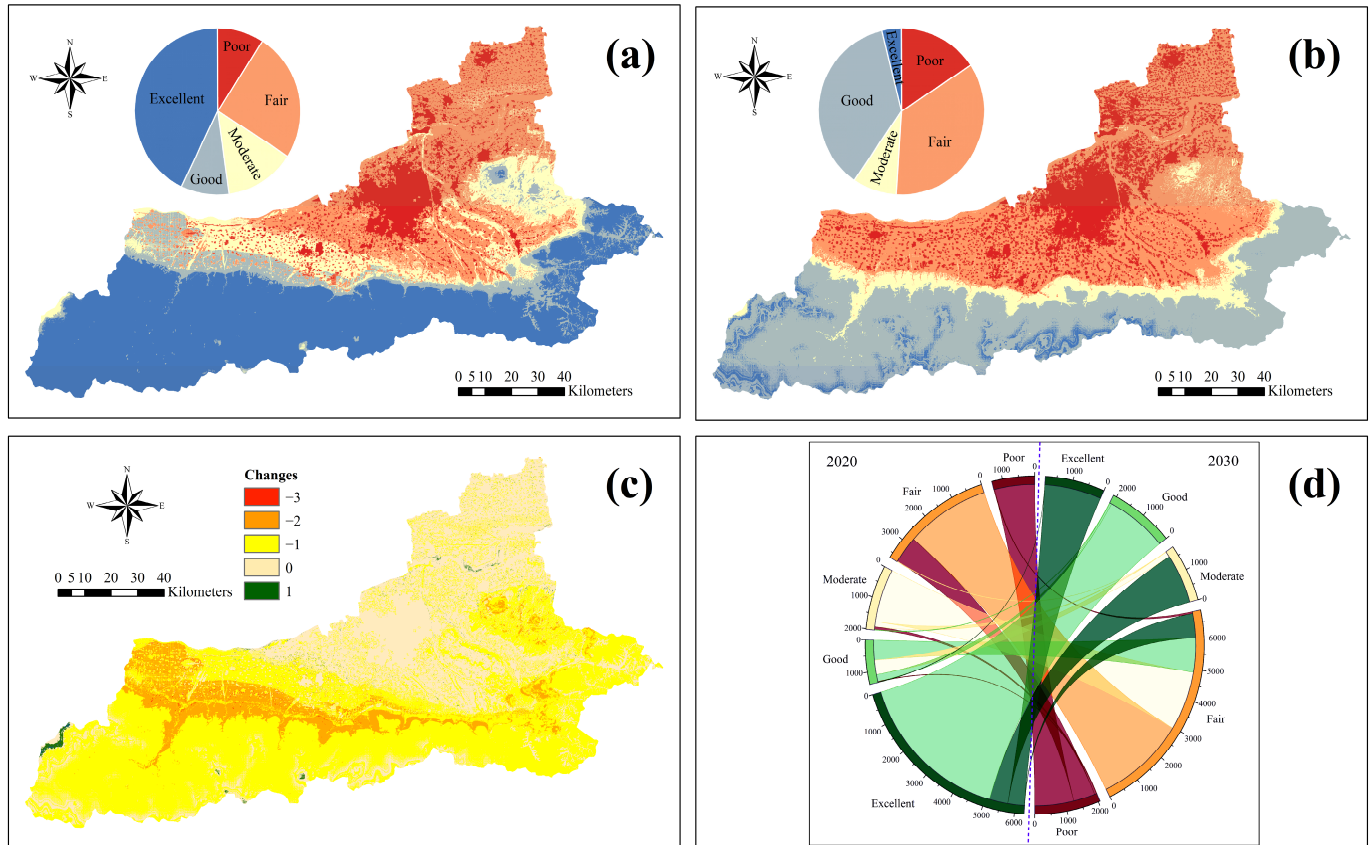


Figure 8. Spatial distribution and change in ecological environment quality levels: (a) ecological levels in 2020; (b) ecological levels in 2030; (c) spatial changes; (d) quantitative changes.

Similarly, we divided the GISEI in 2030 into five levels with the same breakpoint values. The result is shown in Figure 8b. Overall, the distribution of the ecological environment quality in Xi’an in this period was still better in the southern Qinling Mountains than in the Guanzhong Plain, but the ecological environment quality had seriously deteriorated compared with that in 2020, in which the excellent areas accounted for only 3.8%, a decrease of 39%. However, the fair areas increased significantly from 25% to 35.3%, and the Guanzhong Plain areas were almost all fair or even poor, and the proportion of poor, moderate, and good was 15.7%, 8.6%, and 36.6%, respectively.

We subtracted the GISEI in 2020 and the GISEI in 2030 to obtain the spatial changes in ecological environment quality from 2020 to 2030 (Figure 8c). Here, the values indicate the level of the changes, where a positive value means better, a negative value means worse, and zero means no change. For example, it means that the ecological environment quality has deteriorated by three levels if the value is -3 . There were very few areas with ecological environment quality change for the better or a three-level change for the worse; the areas with no change in ecological quality were mainly in the Guanzhong Plain and the southern part of the Qinling Mountains; the areas with two levels of worsening ecological environment quality were mainly in the areas bordering the Qinling Mountains and the Guanzhong Plain; and the ecological environment quality of most of the Qinling Mountains had degraded by one level.

At the same time, we also examined the area transformation between ecological environment quality levels (Figure 8d). From 2020 to 2030, for poor, 19.78 km² will transform into fair; for fair, 886.94 km² will transform into poor, and 16.42 km² will transform into moderate; for moderate, 89.08 km² will transform into poor, 1747 km² will transform into fair, and 16.65 km² will transform into good; and for good, 16.69 km² will transform into poor, 652.65 km² will transform into fair, 469.97 km² will transform into moderate, and 13.86 km² will transform into excellent; for excellent, 4.61 km² will transform into fair, 611.11 km² will transform into moderate, and 5136.71 km² will transform into good. In summary, only 66.71 km² of the ecological environment quality had changed for the better, while the area that had changed for the worse was as high as 9614.76 km², and moderate and good almost all decreased by one level, while excellent had the most serious change, with more than half of the ecological environment quality deteriorated, and some of them even decreased by three levels.

4. Discussion

4.1. The Advantages and Disadvantages of GISEI

We assessed the ecological environment quality in Xi'an in 2020 using RSEI (Figure 3) and GISEI (Figure 5c), respectively, and it can be seen from the two figures that both RSEI and GISEI identify the ecological environment quality in Xi'an well. However, there is a slight difference in the details; for example, in the central city of Xi'an, the results of the RSEI assessment can distinguish the difference, while the results of the GISEI assessment are almost all shown in red. It seems that the RSEI ecological environment quality can better highlight the details, but the indicators of the RSEI and the GISEI are calculated differently, as far as the buildings are concerned, the RSEI uses the reflectance of remote sensing images to calculate the normalized difference built-up index (NDBI) [48], while the buildings of the GISEI are obtained through supervised classification by machine learning, as well as manual visual interpretation. Therefore, the ecological environment quality assessed by the GISEI is more accurate from the perspective of the indicators data. The RSEI has significant advantages in dynamic monitoring of ecological environment quality. However, it cannot predict future changes in the ecological environment quality and is not suitable for research in large areas. However, the prediction of land use and meteorological data is more mature, and the GISEI can realize the prediction of future ecological environmental quality using land use and meteorological data as ecological indicators and can evaluate over large areas because of the ease of access to such ecological indicator data. In addition, to ensure the accuracy of the model, we chose four popular regression analysis methods, by analyzing the performance of the regression results in different aspects we found that in terms of the standard deviation, Ridge > BP > RF > SVM; in terms of the RMSE, RF > BP > SVM > Ridge; and in terms of the correlation, RF > BP > SVM > Ridge. We chose the RF through comprehensive consideration, this machine learning method has better results, but its readability is not good. With the help of the Ridge regression, we know that the relative humidity, temperature, and construction land are the main factors affecting the ecological environment quality.

A large amount of ecological indicator data at different times need to be collected and processed when we monitor the ecological environment quality dynamically, which is undoubtedly a huge amount of work, unlike the RSEI which can be easily realized with the help of Google Earth Engine. Therefore, the GISEI does not perform well in the dynamic monitoring of an ecological environment. In addition, factors such as population and economy have a greater impact on the ecological environment, and although there is a strong correlation between land use types and these factors, they cannot be completely replaced. Therefore, the GISEI reflects the state of the ecological environment, the same as the RSEI, and does not reflect all the factors affecting the ecological environment or the relationship between these factors.

4.2. The Reasons and Policy Implications

By predicting the ecological environment quality in Xi'an in 2030, we found that there will be a large extent of ecological degradation in Xi'an by 2030, and one of the main reasons for this is that the construction land will have increased by 9% from 2020 to 2030. The densely built areas may cause the land surface temperature to rise and the urban heat island effect, making the city less comfortable in hot weather [49]. Furthermore, numerous buildings divide and destroy the natural landscape, exacerbating the degradation of the ecological environment quality [50]. Another reason is that the climate of Xi'an will become warmer and drier by 2030. If the city's ecological environment continues to deteriorate, plant and animal habitats will be destroyed, urban pollutants will be difficult to clean up, factories will be forced to close down, and the city will lose its population, making it difficult to sustain development when it is a serious threat to the health of its residents. Therefore, we need to protect the ecological environment as early as possible, so that the ecological environment will change for the better or slow down the rate of deterioration.

The ecological environment quality in Xi'an will be seriously deteriorated by 2030 under the natural development scenario. However, Yang [9] dynamically monitored the ecological quality of Xi'an over the past 20 years and showed that the overall ecological quality of Xi'an will first decrease and then increase. The reason for this is that the theory that lucid waters and lush mountains are invaluable assets was proposed in 2005 and implemented nationwide in 2017, which has led to increased protection of the ecosystem. It shows that human policies are crucial to the ecosystem and can even change the direction of ecological quality development. In other words, the future quality of the urban ecosystem depends on our current behavior. If we want to guide the ecological environment quality to continuously develop in a good direction, we need to make great efforts. Compared with previous studies, the advantage of this paper is that by analyzing the future changes in the ecological environment quality, we identify the ecologically fragile areas, which are crucial for the delineation of ecological red line and urban planning and provide spatial references for ecological environment protection and management. We suggest that different measures should be taken in different areas. In areas where the ecological environment is already poor, we should strengthen urban greening and properly dispose of domestic garbage and industrial wastewater; in areas where the ecological environment is excellent, protection should be strengthened. In particular, the development of tourism resources should be moderate and reasonable; and in fragile areas, where protection should be strengthened, the ecological environment may deteriorate, and it is necessary to take some treatment measures, such as establishing water source protection zones, optimizing the soil, planting trees, and so on.

4.3. The Limitations and the Research Topics

The purpose of this paper is to provide a new method for assessing and predicting the ecological environment quality and to demonstrate the feasibility of the GISEI using Xi'an as an example. We have selected only one scenario to predict ecological indicators. However, this prediction is often inaccurate, and a multi-scenario prediction should be carried out in subsequent studies. In addition, the ecological environment is a whole, and cities have to sacrifice the ecological environment for the sake of development. Therefore, the neighboring areas play an important role in ecological compensation, and a large-scale ecological environment quality assessment is essential. Coincidentally, another advantage of the GISEI is that it can be applied to large-scale ecological environmental quality assessments. Therefore, future research should focus on the ecological environment of urban agglomerations and their neighborhoods on a large scale.

5. Conclusions

This paper assesses and predicts the ecological environment quality in Xi'an. Some of the contributions of this paper are calculating the RSEI of Xi'an in 2020, establishing a relationship between the RSEI and ecological indicators using regression analysis, and

assessing the ecological environmental quality of Xi'an in 2020 using the GISEI, which found that the ecological environmental quality of the Qinling Mountains in the southern part of Xi'an is better than that of the plains. The ecological environmental quality is generally better in this period. The proportion of excellent areas is 42.8%.

Another contribution of this paper is that we predicted the ecological environment quality in Xi'an in 2030 through the prediction of ecological indicators. By 2030, the ecological environment quality in Xi'an as a whole will be poor, excellent areas are only 3.8%, and most of the area also shows poor quality, only the ecological environmental quality of the southern Qinling Mountains is still good, but the areas that account for Xi'an's area are relatively small. Meanwhile, we analyzed the changes in the ecological environment quality from 2020 to 2030; the regions with a serious degradation of ecological environment quality are mainly located in the areas bordering the Qinling Mountains and the Guanzhong Plain. The ecological environment quality in most areas of the Qinling Mountains will deteriorate from excellent to good, almost all of the original moderate and good areas will have decreased by one level, and the change in excellent areas is the most significant. In addition, through the assessment and prediction of the ecological environment quality in Xi'an, it is proved that the GISEI ecological environment assessment method proposed in this paper is feasible and has a strong robustness.

Author Contributions: Conceptualization, S.Y.; methodology, S.Y.; software, L.C. and W.W.; validation, W.W.; formal analysis, L.C.; resources, J.J.; writing—original draft preparation, L.C.; writing—review and editing, S.Y.; visualization, L.C.; supervision, S.Y.; project administration, S.Y.; funding acquisition, L.C. and S.Y. All authors have read and agreed to the published version of the manuscript.

Funding: This study is supported by the Excellent Graduate Training Program of Shaanxi Normal University (Grant No. LHRCCX23162) and the National Natural Science Foundation of China (Grant No. 41771110).

Data Availability Statement: Data are contained within the article.

Acknowledgments: The authors are grateful for the financial support provided by the Excellent Graduate Training Program of Shaanxi Normal University and the National Natural Science Foundation of China. Thank you to all anonymous reviewers and editors for their comments and help.

Conflicts of Interest: The authors declare no conflicts of interest.

References

1. Lin, X.; Lu, C.; Song, K.; Su, Y.; Lei, Y.; Zhong, L.; Gao, Y. Analysis of Coupling Coordination Variance between Urbanization Quality and Eco-Environment Pressure: A Case Study of the West Taiwan Strait Urban Agglomeration, China. *Sustainability* **2020**, *12*, 2643. [[CrossRef](#)]
2. Ji, J.; Wang, S.; Zhou, Y.; Liu, W.; Wang, L. Spatiotemporal Change and Landscape Pattern Variation of Eco-Environmental Quality in Jing-Jin-Ji Urban Agglomeration From 2001 to 2015. *IEEE Access* **2020**, *8*, 125534–125548. [[CrossRef](#)]
3. Wang, Z.; Lyu, L.; Liu, W.; Liang, H.; Huang, J.; Zhang, Q.-B. Topographic patterns of forest decline as detected from tree rings and NDVI. *Catena* **2021**, *198*, 105011. [[CrossRef](#)]
4. Zhang, F.; Xing, Z.; Zhao, C.; Deng, J.; Yang, B.; Tian, Q.; Rees, H.W.; Badreldin, N. Characterizing long-term soil and water erosion and their interactions with various conservation practices in the semi-arid Zulihe basin, Dingxi, Gansu, China. *Ecol. Eng.* **2017**, *106*, 458–470. [[CrossRef](#)]
5. Zhao, G.; Mu, X.; Wen, Z.; Wang, F.; Gao, P. Soil Erosion, Conservation, and Eco-Environment Changes in the Loess Plateau of China. *Land Degrad. Dev.* **2013**, *24*, 499–510. [[CrossRef](#)]
6. Dai, X.; Gao, Y.; He, X.; Liu, T.; Jiang, B.; Shao, H.; Yao, Y. Spatial-temporal pattern evolution and driving force analysis of ecological environment vulnerability in Panzhihua City. *Environ. Sci. Pollut. Res.* **2020**, *28*, 7151–7166. [[CrossRef](#)] [[PubMed](#)]
7. Boori, M.S.; Choudhary, K.; Paringer, R.; Kupriyanov, A. Eco-environmental quality assessment based on pressure-state-response framework by remote sensing and GIS. *Remote Sens. Appl. Soc. Environ.* **2021**, *23*, 100530. [[CrossRef](#)]
8. Yang, X.Y.; Meng, F.; Fu, P.J.; Wang, Y.Q.; Liu, Y.H. Time-frequency optimization of RSEI: A case study of Yangtze River Basin. *Ecol. Indic.* **2022**, *141*, 109080. [[CrossRef](#)]
9. Yang, S.; Su, H. Evaluation of Urban Ecological Environment Quality Based on Google Earth Engine: A Case Study in Xi'an, China. *Pol. J. Environ. Stud.* **2023**, *32*, 927–942. [[CrossRef](#)]
10. Wang, S.; Zhang, M.; Xi, X. Ecological Environment Evaluation Based on Remote Sensing Ecological Index: A Case Study in East China over the Past 20 Years. *Sustainability* **2022**, *14*, 5771. [[CrossRef](#)]

11. Jing, Y.Q.; Zhang, F.; He, Y.F.; Kung, H.T.; Johnson, V.C.; Arikena, M. Assessment of spatial and temporal variation of ecological environment quality in Ebinur Lake Wetland National Nature Reserve, Xinjiang, China. *Ecol. Indic.* **2020**, *110*, 105874. [[CrossRef](#)]
12. Gao, P.W.; Kasimu, A.; Zhao, Y.Y.; Lin, B.; Chai, J.P.; Ruzi, T.; Zhao, H.M. Evaluation of the Temporal and Spatial Changes of Ecological Quality in the Hami Oasis Based on RSEI. *Sustainability* **2020**, *12*, 7716. [[CrossRef](#)]
13. Hird, J.N.; McDermid, G.J. Noise reduction of NDVI time series: An empirical comparison of selected techniques. *Remote Sens. Environ.* **2009**, *113*, 248–258. [[CrossRef](#)]
14. LeVine, D.; Crews, K. Time series harmonic regression analysis reveals seasonal vegetation productivity trends in semi-arid savannas. *Int. J. Appl. Earth Obs.* **2019**, *80*, 94–101. [[CrossRef](#)]
15. Xiong, Y.; Xu, W.H.; Lu, N.; Huang, S.D.; Wu, C.; Wang, L.G.; Dai, F.; Kou, W.L. Assessment of spatial-temporal changes of ecological environment quality based on RSEI and GEE: A case study in Erhai Lake Basin, Yunnan province, China. *Ecol. Indic.* **2021**, *125*, 107518. [[CrossRef](#)]
16. Feng, Y.; Yang, Q.; Tong, X.; Chen, L. Evaluating land ecological security and examining its relationships with driving factors using GIS and generalized additive model. *Sci. Total Environ.* **2018**, *633*, 1469–1479. [[CrossRef](#)] [[PubMed](#)]
17. Marull, J.; Pino, J.; Mallarach, J.M.; Cordobilla, M.J. A Land Suitability Index for Strategic Environmental Assessment in metropolitan areas. *Landsc. Urban Plan.* **2007**, *81*, 200–212. [[CrossRef](#)]
18. Robati, M.; Monavari, S.M.; Majedi, H. Urban Environment Quality Assessment by Using Composite Index Model. *Environ. Prog. Sustain.* **2015**, *34*, 1473–1480. [[CrossRef](#)]
19. Yang, X.; Meng, F.; Fu, P.; Zhang, Y.; Liu, Y. Spatiotemporal change and driving factors of the Eco-Environment quality in the Yangtze River Basin from 2001 to 2019. *Ecol. Indic.* **2021**, *131*, 108214. [[CrossRef](#)]
20. McDonnell, M.J.; MacGregor-Fors, I. The ecological future of cities. *Science* **2016**, *352*, 936–938. [[CrossRef](#)]
21. Tang, H.; Fang, J.; Xie, R.; Ji, X.; Li, D.; Yuan, J. Impact of Land Cover Change on a Typical Mining Region and Its Ecological Environment Quality Evaluation Using Remote Sensing Based Ecological Index (RSEI). *Sustainability* **2022**, *14*, 12694. [[CrossRef](#)]
22. Curran, G. Ecological modernisation and climate change in Australia. *Environ. Polit.* **2009**, *18*, 201–217. [[CrossRef](#)]
23. Wu, S.P.; Gao, X.; Lei, J.Q.; Zhou, N.; Guo, Z.K.; Shang, B.J. Ecological environment quality evaluation of the Sahel region in Africa based on remote sensing ecological index. *J. Arid Land* **2022**, *14*, 14–33. [[CrossRef](#)]
24. Sun, C.; Li, J.L.; Liu, Y.C.; Cao, L.D.; Zheng, J.H.; Yang, Z.J.; Ye, J.W.; Li, Y. Ecological quality assessment and monitoring using a time-series remote sensing-based ecological index (ts-RSEI). *Giscience Remote Sens.* **2022**, *59*, 1793–1816. [[CrossRef](#)]
25. Liu, K.; Zhang, C.Z.; Zhang, H.; Xu, H.; Xia, W. Spatiotemporal Variation and Dynamic Simulation of Ecosystem Carbon Storage in the Loess Plateau Based on PLUS and InVEST Models. *Land* **2023**, *12*, 1065. [[CrossRef](#)]
26. Rong, T.Q.; Zhang, P.Y.; Zhu, H.R.; Jiang, L.; Li, Y.Y.; Liu, Z.Y. Spatial correlation evolution and prediction scenario of land use carbon emissions in China. *Ecol. Inf.* **2022**, *71*, 101802. [[CrossRef](#)]
27. Li, L.; Chen, Z.C.; Wang, S.D. Optimization of Spatial Land Use Patterns with Low Carbon Target: A Case Study of Sanmenxia, China. *Int. J. Environ. Res. Pub. Health* **2022**, *19*, 14178. [[CrossRef](#)] [[PubMed](#)]
28. Zamani, Y.; Monfared, S.A.H.; Moghaddam, M.A.; Hamidianpour, M. A comparison of CMIP6 and CMIP5 projections for precipitation to observational data: The case of Northeastern Iran. *Theor. Appl. Climatol.* **2020**, *142*, 1613–1623. [[CrossRef](#)]
29. Zhang, W.J.; Zhang, X.Y.; Wang, H. The Role of Aerosol-Radiation Interaction in the Meteorology Prediction at the Weather Scale in the Numerical Weather Prediction Model. *Geophys. Res. Lett.* **2022**, *49*, e2021GL097026. [[CrossRef](#)]
30. Xiao, Z.N.; Liu, B.; Liu, H.; Zhang, D. Progress in climate prediction and weather forecast operations in China. *Adv. Atmos. Sci.* **2012**, *29*, 943–957. [[CrossRef](#)]
31. Simpkins, G. Progress in climate modelling. *Nat. Clim. Chang.* **2017**, *7*, 684–686. [[CrossRef](#)]
32. Eyring, V.; Bony, S.; Meehl, G.A.; Senior, C.A.; Stevens, B.; Stouffer, R.J.; Taylor, K.E. Overview of the Coupled Model Intercomparison Project Phase 6 (CMIP6) experimental design and organization. *Geosci. Model Dev.* **2016**, *9*, 1937–1958. [[CrossRef](#)]
33. Ding, Y.; Peng, S. Spatiotemporal change and attribution of potential evapotranspiration over China from 1901 to 2100. *Theor. Appl. Climatol.* **2021**, *145*, 79–94. [[CrossRef](#)]
34. Airiken, M.; Li, S.C. The Dynamic Monitoring and Driving Forces Analysis of Ecological Environment Quality in the Tibetan Plateau Based on the Google Earth Engine. *Remote Sens.* **2024**, *16*, 682. [[CrossRef](#)]
35. Abson, D.J.; Dougill, A.J.; Stringer, L.C. Using Principal Component Analysis for information-rich socio-ecological vulnerability mapping in Southern Africa. *Appl. Geogr.* **2012**, *35*, 515–524. [[CrossRef](#)]
36. Jimenez-Munoz, J.C.; Sobrino, J.A.; Skokovic, D.; Mattar, C.; Cristobal, J. Land Surface Temperature Retrieval Methods From Landsat-8 Thermal Infrared Sensor Data. *IEEE Geosci. Remote Sens. Lett.* **2014**, *11*, 1840–1843. [[CrossRef](#)]
37. Sekertekin, A.; Bonafoni, S. Land Surface Temperature Retrieval from Landsat 5, 7, and 8 over Rural Areas: Assessment of Different Retrieval Algorithms and Emissivity Models and Toolbox Implementation. *Remote Sens.* **2020**, *12*, 294. [[CrossRef](#)]
38. Uyanik, G.K.; Güler, N. A Study on Multiple Linear Regression Analysis. *Procedia—Soc. Behav. Sci.* **2013**, *106*, 234–240. [[CrossRef](#)]
39. Kibria, B.M.G.; Månsson, K.; Shukur, G. Performance of Some Logistic Ridge Regression Estimators. *Comput. Econ.* **2011**, *40*, 401–414. [[CrossRef](#)]
40. Brereton, R.G.; Lloyd, G.R. Support Vector Machines for classification and regression. *Analyst* **2010**, *135*, 230–267. [[CrossRef](#)]
41. Li, Y.; Zou, C.; Bercibar, M.; Nanini-Maury, E.; Chan, J.C.W.; van den Bossche, P.; Van Mierlo, J.; Omar, N. Random forest regression for online capacity estimation of lithium-ion batteries. *Appl. Energy* **2018**, *232*, 197–210. [[CrossRef](#)]

42. Chen, F.; Han, S.; Xu, J.; Yan, M.; Liu, Z. Using multiple linear regression and BP neural network to predict critical meteorological conditions of expressway bridge pavement icing. *PLoS ONE* **2022**, *17*, e0263539. [[CrossRef](#)] [[PubMed](#)]
43. Taylor, K.E. Summarizing multiple aspects of model performance in a single diagram. *J. Geophys. Res.* **2001**, *106*, 7183–7192. [[CrossRef](#)]
44. Tang, Q.; Dai, J.; Liu, J.; Liu, C.; Liu, Y.; Ren, C. Quantitative detection of defects based on Markov–PCA–BP algorithm using pulsed infrared thermography technology. *Infrared Phys. Technol.* **2016**, *77*, 144–148. [[CrossRef](#)]
45. Luo, H.; Li, Y.; Gao, X.; Meng, X.; Yang, X.; Yan, J. Carbon emission prediction model of prefecture-level administrative region: A land-use-based case study of Xi’an city, China. *Appl. Energy* **2023**, *348*, e0263539. [[CrossRef](#)]
46. Liang, X.; Guan, Q.; Clarke, K.C.; Liu, S.; Wang, B.; Yao, Y. Understanding the drivers of sustainable land expansion using a patch-generating land use simulation (PLUS) model: A case study in Wuhan, China. *Comput. Environ. Urban Syst.* **2021**, *85*, 101569. [[CrossRef](#)]
47. Ye, H.; Song, Y.Y.; Xue, D.Q. Multi-Scenario Simulation of Land Use and Habitat Quality in the Guanzhong Plain Urban Agglomeration, China. *Int. J. Environ. Res. Pub. Health* **2022**, *19*, 8703. [[CrossRef](#)] [[PubMed](#)]
48. Xu, H. A new index for delineating built-up land features in satellite imagery. *Int. J. Remote Sens.* **2008**, *29*, 4269–4276. [[CrossRef](#)]
49. Radhi, H.; Fikry, F.; Sharples, S. Impacts of urbanisation on the thermal behaviour of new built up environments: A scoping study of the urban heat island in Bahrain. *Landsc. Urban Plan.* **2013**, *113*, 47–61. [[CrossRef](#)]
50. Godefroid, S.; Koedam, N. Urban plant species patterns are highly driven by density and function of built-up areas. *Landsc. Ecol.* **2007**, *22*, 1227–1239. [[CrossRef](#)]

Disclaimer/Publisher’s Note: The statements, opinions and data contained in all publications are solely those of the individual author(s) and contributor(s) and not of MDPI and/or the editor(s). MDPI and/or the editor(s) disclaim responsibility for any injury to people or property resulting from any ideas, methods, instructions or products referred to in the content.